

Three-Dimensional Hybrid Framework Containing U_2O_{13} Dimers Connected via Cation–Cation Interactions

Rachel C. Severance, Mark D. Smith, and Hans-Conrad zur Loye*

Department of Chemistry and Biochemistry, University of South Carolina, 631 Sumter Street, Columbia, South Carolina 29208, United States

S Supporting Information

ABSTRACT: A three-dimensional metal–organic framework with cation–cation interactions, $UO_2(NO_2TA)_2(H_2O)$ (**1**), was synthesized hydrothermally and characterized via single-crystal X-ray diffraction, powder X-ray diffraction, UV–vis spectroscopy, and fluorescence spectroscopy ($NO_2TA = 2$ -nitroterephthalic acid). **1** crystallizes in the monoclinic space group $P2_1/n$ [$a = 11.6970(7)$ Å, $b = 15.1449(9)$ Å, $c = 12.2564(8)$ Å, and $\beta = 109.193(1)^\circ$] and contains U_2O_{13} dimers. The UV–vis spectrum of **1** contains peaks attributable to both the ligand and the uranium cation. Furthermore, the ligand and the uranium cation of **1** can be independently excited, giving rise to two different luminescent spectra.

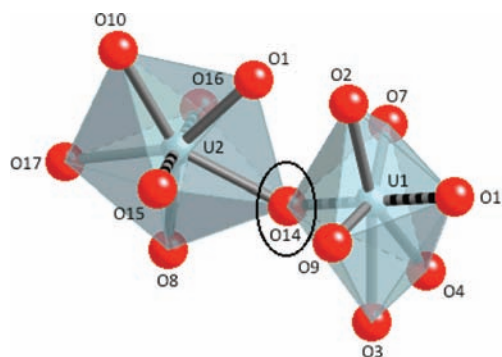


Figure 1. Coordination environment about U1 and U2, detailing the CCI via the bridging oxide ligand (O14). Equatorial U–O bonds = solid gray, and axial U–O bonds = black/gray.

There has been significant interest in the creation of new metal–organic hybrid materials containing the uranyl species (UO_2^{2+}).¹ Typically, two-dimensional or lower structures are obtained, in part, because of the constraints of the uranyl metal center. It is, of course, possible to create three-dimensional (3D) structures if the linking ligand is multidentate and appropriately cross-links the uranyl centers. In most structures containing the uranyl moiety, the axial sites of the uranium(VI) cation are occupied by the two terminal oxide atoms, while the equatorial sites connect up to six ligands in the equatorial plane.² As a result, the uranyl metal site generally assumes bipyramidal geometries and the connectivity between the uranyl centers leads to the formation of lower dimensional structures.³

In contrast, the extended 3D structure of $UO_2(NO_2TA)_2 \cdot (H_2O)$ (**1**) contains two distinct uranium sites that are connected via cation–cation interactions (CCIs), in which an axial oxide atom belonging to U1 is occupying an equatorial site belonging to U2. This creates an oxo-bridged dimer with a nonterminal axial oxide ligand (Figure 1). One result of this bridging behavior is that the bond lengths for O14 are noticeably lengthened, consistent with the weakening of the U–O bonds in this arrangement.

While much more common in pentavalent actinyl chemistry,^{4,5} CCIs occur in relatively few hexavalent uranium compounds. Some of the cases with uranium(VI) have been found in mixed-valent species involving a pentavalent ion.^{5,6} The low reactivity of the axial oxide ligand in the UO_2^{2+} ion has been attributed to the lower basicity of the UO_2^{2+} oxygen atoms.^{6,7} Despite their rarity, the CCIs serve to increase dimensionality within solid-state structures in almost all cases when present.

In contrast to the small number of uranium(VI) cations connected via CCIs into systems ranging from trimers to fully interconnected polyhedra,^{5,7–9} an even rarer case is that of dimeric formations.⁹ In this particular case, the dimers are further connected via their bridging organic ligands, NO_2TA , without the presence of alkali- or alkaline-earth-metal cations.¹⁰

The formation of these CCIs within this structure is also in contrast to coordination of the uranyl cation to similar benzene dicarboxylate derivatives, which typically form layered structures.¹¹

Crystals of **1** were hydrothermally synthesized under autogenous pressure as yellow plates in 50% yield based on stoichiometric ratios. *Caution: Uranyl acetate contains depleted uranium, but standard precautions for handling radioactive and highly toxic substances should be followed.*

The structure of a yellow plate-shaped single crystal of **1** was determined at 100 K and found to crystallize in the space group $P2_1/n$, as determined by the pattern of systematic absences in the intensity data. As shown in Figure 2, the asymmetric unit consists of two distinct UO_2 groups (centered around U1 and U2), two distinct NO_2TA ligands (L1 and L2), and one water molecule. The purity of the bulk material was verified via powder X-ray diffraction (see Figure S1 in the Supporting Information).

The two uranium sites are linked via an oxide ligand into a U1–U2 dimer arrangement, which are further linked to neighboring U1–U2 dimers via the NO_2TA ligands. Specifically, U1 has one terminal axial oxide ligand [U1–O13 = 1.756(5) Å] and

Received: May 10, 2011

Published: August 04, 2011

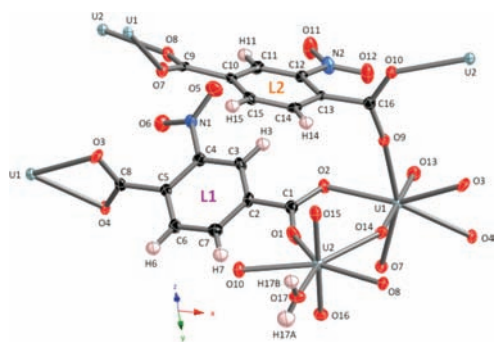


Figure 2. Asymmetric unit of **1**, with additional atoms to complete the coordination spheres. Displacement ellipsoids drawn at the 50% probability level.

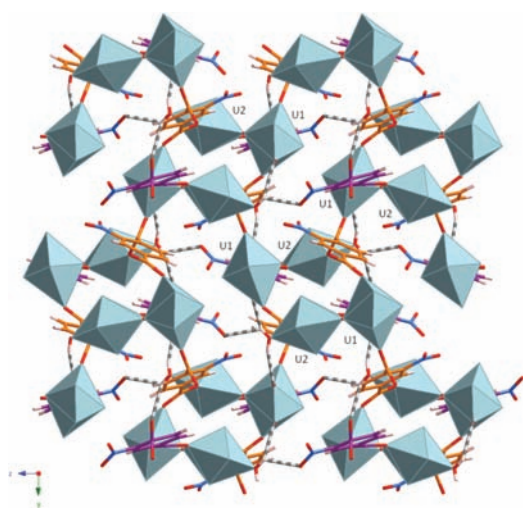


Figure 3. Overall 3D motif of **1**. L1 = purple, and L2 = orange.

one bridging axial oxide ligand, which occupies an equatorial site on U2 [U1–O14 = 1.808(5) Å; U2–O14 = 2.506(5) Å]. U2 has two terminal axial oxide ligands [U2–O15 = 1.752(5) Å; U2–O16 = 1.758(5) Å] and a terminal equatorial water molecule connected via O17 [U2–O17 = 2.361(5) Å]. This water molecule forms hydrogen bonds to a neighboring ligand (L1) via H17A and a nitro oxygen atom (O5) [O17–H17A···O5 = 2.25(7) Å]. The water molecule also forms hydrogen bonds to a second and third neighboring ligand (both L1) via carboxylate oxygen atoms (O3 and O4) [O17–H17B···O3 = 2.01(5) Å; O17–H17A···O4 = 2.25(7) Å]. The hydrogen-bonding environment around the water molecule is shown in Figure S2 in the Supporting Information.

There are two different ligand binding motifs in this structure, schematically shown in Figure 2 and S3. L1 and L2 are linked to three and four different uranyl centers, respectively, contributing to the three-dimensionality of this structure.

The overall network of **1** is shown in Figure 3. In this framework, U1 binds to four separate NO₂TA ligands: two L1 and two L2. The first ligand (L1) binds via both oxygen atoms of one carboxylate group (O3, O4). The second ligand (L1) binds to U1 via one oxygen atom (O2) of a carboxylate group, with the other oxygen atom (O1) of the same group binding to U2. The third ligand (L2) binds to U1 via one oxygen atom (O7) of a

carboxylate group, with the other oxygen atom (O8) of the same group binding to U2 in a neighboring U1–U2 dimer. The fourth ligand (L2) binds to U1 via one oxygen atom (O9) of a carboxylate group, with the other oxygen atom (O10) of the same group binding to U2 in a neighboring U1–U2 dimer.

U2 binds to three separate NO₂TA ligands: one L1 and two L2. L1 is also linked to U1, and bridges U1 and U2 within one dimer via O2 and O1, respectively. The second ligand (L2) binds to U2 via one oxygen atom (O8) of a carboxylate group, with the other oxygen atom (O7) of the same group binding to U1 in a neighboring U1–U2 dimer. The third ligand (L2) binds to U2 via one oxygen atom (O10) of a carboxylate group, with the other oxygen atom (O9) of the same group binding to U1 in a neighboring U1–U2 dimer.

A detailed discussion of the valence bond strengths for each bond is included in the Supporting Information. In summary, U2 has a bond valence sum of 6.08, consistent with the assigned oxidation state of 6+. The bond valence sum of the five equatorial ligands accounts for 2.07 of the bond valence and that of the two axial oxygen atoms (O15 and O16) account for 4.01, as expected for a normal uranyl species. For U1, the bond valence sum is 6.04, consistent with the assigned oxidation state of 6+. However, because of the sharing of one of the axial oxygen atoms (O14) with U1, we expect the bond valence for O14 to be less. In fact, the five equatorial ligands account for 2.19 of the bond valence sum for uranium, slightly more than that found for U2. The unshared axial oxygen (O13) accounts for a bond valence sum of 2.00, while the shared axial oxygen (O14) is underbonded with a bond valence sum of only 1.84. This is consistent with what one expects for CCI₅.⁵ In accordance with this theory, the bond distances for the axial oxygen atoms, U1–O13, U2–O15, and U2–O16, are normal with lengths of 1.756(5), 1.752(5), and 1.758(5) Å, respectively, while the bond distance for the shared axial oxygen U1–O14 is noticeably longer at 1.808(5) Å, as expected for that being shared with another uranium center.

In addition to the interesting structural morphology, the photoluminescence in this framework is also unusual. Despite the quenching character of the nitro group¹² and the CCI, **1** displays the characteristic five- to six-band luminescence pattern (Figures 4 and 5) due to the character of the uranyl group as a strong emitter. When **1** is excited at 236 nm, an emission is observed at 403 nm, which is blue-shifted by approximately

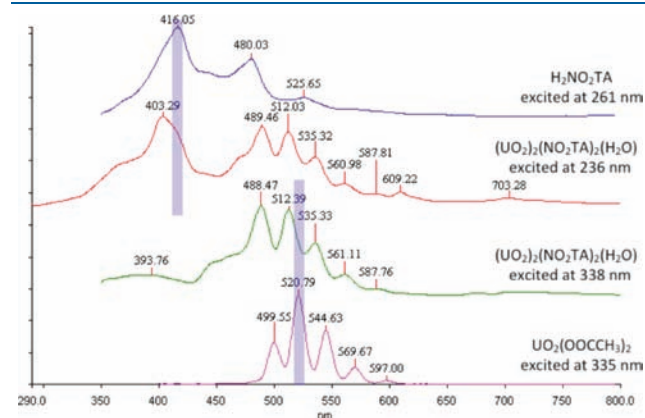


Figure 4. Emission spectra of **1** upon excitation in the ligand region (red) and the uranyl region (green), compared to the ligand emission (blue) and the uranyl acetate emission (purple).

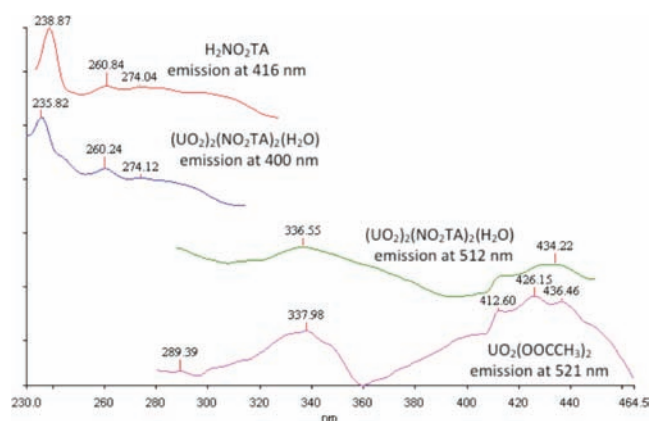


Figure 5. Excitation spectra of **1** [$(\text{UO}_2)_2(\text{NO}_2\text{TA})_2(\text{H}_2\text{O})$], the ligand [$\text{H}_2\text{NO}_2\text{TA}$], and uranyl acetate [$\text{UO}_2(\text{OOCH}_3)_2$].

13 nm from the corresponding peak in the emission spectra of the $\text{H}_2\text{NO}_2\text{TA}$ ligand alone. It follows that both the complex and ligand have similar excitation spectra when measured with the emission set to the 400 nm region. When **1** is excited at 338 nm instead, the uranyl's characteristic five-band emission pattern, plus a shoulder, is observed centered at 512 nm, which is blue-shifted by approximately 8 nm relative to the corresponding five-band emission pattern in the spectrum of uranyl acetate. Clearly, both the complex and uranyl acetate have similar excitation spectra when measured with the emission set to the appropriate region. Furthermore, the UV–vis absorbance spectrum of **1** includes peaks in both the 350 and 430 regions, corresponding to absorbance peaks in the $\text{H}_2\text{NO}_2\text{TA}$ and uranyl acetate spectra, respectively (Figure S4).

In summary, the unique axial–equatorial oxo-bridged dimer arrangement of **1** was achieved, where cation–cation interactions between the uranyl centers assist in the formation of the 3D framework of this material.

ASSOCIATED CONTENT

S Supporting Information. X-ray crystallographic experimental details, bond angles and distances, hydrogen-bonding distances, powder X-ray diffraction details, and crystallographic data in CIF format. This material is available free of charge via the Internet at <http://pubs.acs.org>. CIF data are also available through Cambridge Crystallographic Data Centre as supplementary publication CCDC 824258 and can be obtained free of charge via www.ccdc.cam.ac.uk/data-request/cif, by e-mailing data_request@ccdc.cam.ac.uk, or by contacting The Cambridge Crystallographic Data Centre, 12 Union Road, Cambridge CB2 1EZ, U.K.; fax +44 1223 336033.

AUTHOR INFORMATION

Corresponding Author

*E-mail: zurloye@mail.chem.sc.edu. Tel: +1-803-777-6916. Fax: +1-803-777-8508.

ACKNOWLEDGMENT

Financial support from the NSF through Grant CHE-0714439 is gratefully acknowledged.

REFERENCES

- (1) (a) Severance, R. C.; Vaughn, S. A.; Smith, M. D.; zur Loye, H.-C. *Solid State Sci.* **2011**, *13*, 1344–1353. (b) Henry, N.; Lagrenée, M.; Loiseau, T.; Clavier, N.; Dacheux, N.; Abraham, F. *Inorg. Chem. Commun.* **2011**, *14* (2), 429–432. (c) Lhoste, J.; Henry, N.; Roussel, P.; Loiseau, T.; Abraham, F. *Dalton Trans.* **2011**, *40*, 2422–2424. (d) Adelani, P. O.; Albrecht-Schmitt, T. E. *Inorg. Chem.* **2010**, *49* (12), 5701–5705. (e) Rowland, C. E.; Cahill, C. L. *Inorg. Chem.* **2010**, *49* (14), 6716–6724. (f) Thuery, P. *CrystEngComm* **2010**, *12* (6), 1905–1911. (g) Nelson, A.-G. D.; Bray, T. H.; Stanley, F. A.; Albrecht-Schmitt, T. E. *Inorg. Chem.* **2009**, *48* (10), 4530–4535. (h) Ling, J.; Sigmon, G. E.; Burns, P. C. *J. Solid State Chem.* **2009**, *182* (2), 402–408. (i) Thuery, P. *Cryst. Growth Des.* **2008**, *8* (11), 4132–4143. (j) McCleskey, T. M.; Burns, C. J.; Tumas, W. *Inorg. Chem.* **1999**, *38*, 5924–5925. (k) Yagoubi, S.; Obbade, S.; Saad, S.; Abraham, F. *J. Solid State Chem.* **2011**, *184* (5), 971–981.
- (2) Formosinho, S. J.; Burrows, H. D.; Miguel, M. D. G.; Azenha, M. E. D. G.; Saraiva, I. M.; Ribeiro, A. C. D. N.; Khudyakov, I. V.; Gasanov, R. G.; Bolte, M.; Sarakha, M. *Photochem. Photobiol. Sci.* **2003**, *2* (5), 569–575.
- (3) Cahill, C. L.; De Lill, D. T.; Frisch, M. *CrystEngComm* **2007**, *9* (1), 15–26.
- (4) (a) Arnold, P. L.; Hollis, E.; White, F. J.; Magnani, N.; Caciuffo, R.; Love, J. B. *Angew. Chem., Int. Ed.* **2011**, *50* (4), 887–890. (b) Takao, K.; Kato, M.; Takao, S.; Nagasawa, A.; Bernhard, G.; Hennig, C.; Ikeda, Y. *Inorg. Chem.* **2010**, *49* (5), 2349–2359. (c) Mougél, V.; Horeglad, P.; Nocton, G.; Pécaut, J.; Mazzanti, M. *Chem.—Eur. J.* **2010**, *16* (48), 14365–14377. (d) Spencer, L. P.; Schelter, E. J.; Yang, P.; Gdula, R. L.; Scott, B. L.; Thompson, J. D.; Kiplinger, J. L.; Batista, E. R.; Boncella, J. M. *Angew. Chem., Int. Ed.* **2009**, *48* (21), 3795–3798. (e) Skanthakumar, S.; Antonio, M. R.; Soderholm, L. *Inorg. Chem.* **2008**, *47*, 4591–4595. (f) Nocton, G.; Horeglad, P.; Pécaut, J.; Mazzanti, M. *J. Am. Chem. Soc.* **2008**, *130* (49), 16633–16645. (g) Burdet, F.; Pécaut, J.; Mazzanti, M. *J. Am. Chem. Soc.* **2006**, *128* (51), 16512–16513. (h) Albrecht-Schmitt, T. E.; Almond, P. M.; Sykora, R. E. *Inorg. Chem.* **2003**, *42* (12), 3788–3795. (i) Almond, P. M.; Sykora, R. E.; Skanthakumar, S.; Soderholm, L.; Albrecht-Schmitt, T. E. *Inorg. Chem.* **2004**, *43* (3), 958–963. (j) Ewing, R. C.; Runde, W.; Albrecht-Schmitt, T. E. *MRS Bull.* **2010**, *35* (11), 859–866. (k) Wang, S.; Alekseev, E. V.; Miller, H. M.; Depmeier, W.; Albrecht-Schmitt, T. E. *Inorg. Chem.* **2010**, *49* (21), 9755–9757.
- (5) Krot, N. N.; Grigoriev, M. S. *Russ. Chem. Rev.* **2004**, *73* (1), 89–100.
- (6) Mougél, V.; Horeglad, P.; Nocton, G.; Pécaut, J.; Mazzanti, M. *Angew. Chem., Int. Ed.* **2009**, *48* (45), 8477–8480.
- (7) Morrison, J. M.; Moore-Shay, L. J.; Burns, P. C. *Inorg. Chem.* **2011**, *50* (6), 2272–2277.
- (8) (a) Sullens, T. A.; Jensen, R. A.; Shvareva, T. Y.; Albrecht-Schmitt, T. E. *J. Am. Chem. Soc.* **2004**, *126* (9), 2676–2677. (b) Alekseev, E. V.; Krivovichev, S. V.; Depmeier, W.; Siidra, O. I.; Knorr, K.; Suleimanov, E. V.; Chuprunov, E. V. *Angew. Chem., Int. Ed.* **2006**, *43*, 7233–7235. (c) Alekseev, E. V.; Krivovichev, S. V.; Malcherek, T.; Depmeier, W. *Inorg. Chem.* **2007**, *46*, 8442–8444. (d) Kubatko, K.-A.; Burns, P. C. *Inorg. Chem.* **2006**, *45* (25), 10277–10281. (e) Sarsfield, M. J.; Helliwell, M. *J. Am. Chem. Soc.* **2004**, *126*, 1036–1037. (f) Burns, P. C.; Ikeda, Y.; Czerwinski, K. *MRS Bull.* **2010**, *35* (11), 868–876. (g) Mihalcea, I.; Henry, N.; Clavier, N.; Dacheux, N.; Loiseau, T. *Inorg. Chem.* **2011**, *50*, 6243–6249.
- (9) Alekseev, E. V.; Krivovichev, S. V.; Depmeier, W. *J. Solid State Chem.* **2009**, *182* (11), 2977–2984.
- (10) Fortier, S.; Hayton, T. W. *Coord. Chem. Rev.* **2010**, *254* (3–4), 197–214.
- (11) Go, Y. B.; Wang, X.; Jacobson, A. J. *Inorg. Chem.* **2007**, *46*, 6594–6600. Wibowo, A. C.; Smith, M. D.; zur Loye, H.-C. *Chem. Commun.* **2011**, 7371–7373.
- (12) Wibowo, A. C.; Smith, M. D.; zur Loye, H.-C. *CrystEngComm* **2011**, *13* (2), 426–429.